

### LIMNOLOGY and OCEANOGRAPHY



Limnol. Oceanogr. 68, 2023, 2632–2641
© 2023 The Authors. Limnology and Oceanography published by Wiley Periodicals LLC on behalf of Association for the Sciences of Limnology and Oceanography.

doi: 10.1002/lnp.12465

# Model of mesopelagic fish predation on eggs and larvae shows benefits of tuna spawning under full moon

Daniel Ottmann <sup>0</sup>, <sup>1,2\*</sup> Tom J. Langbehn <sup>0</sup>, <sup>3</sup> Patricia Reglero, <sup>2</sup> Diego Alvarez-Berastegui, <sup>2</sup> Øyvind Fiksen <sup>3</sup>

<sup>1</sup>National Institute of aquatic Resources, Technical University of Denmark (DTU-Aqua), Kongens Lyngby, Denmark

#### **Abstract**

Most mesopelagic fish are small planktivores that migrate up at nightfall to feed in the safety of darkness and descend to depth at dawn to escape visual predators. However, the trophic roles can reverse since mesopelagic fishes also predate eggs and larvae of their predators. We use the Atlantic bluefin tuna as a model species to test the hypothesis that fishes in the open ocean synchronize spawning to moon-lit nights (when mesopelagic fishes avoid near-surface waters) to increase offspring fitness. Our analysis over two decades of field observations shows that tuna spawn most intensively the week before full moon. This fits predictions from a mechanistic model where spawning around full moon increases offspring fitness by two orders of magnitude due to low predation from mesopelagic fishes. Circalunar patterns of food availability can also favor fitness of offspring spawned the days before full moon. Our findings suggest that mesopelagic fishes may have an important impact on pelagic fish through predation of early life stages and cause an evolutionary drive to synchronize spawning to the lunar cycle.

The moon affects life on Earth through nighttime illumination and cyclic tides. This creates predictable conditions that can be exploited by organisms to maximize fitness (Fryer 1986; Kronfeld-Schor et al. 2013; Palmer et al. 2017). For instance, some birds and mammals modify their foraging behavior in moon-lit nights to increase feeding success (predators) or reduce predator encounters (prey) (Mougeot and Bretagnolle 2000; Jetz et al. 2003; Prugh and Golden 2014). Some reef invertebrates (Richmond and Hunter 1990; Žuljević et al. 2018; Neely and Butler 2020) and fishes (Takemura et al. 2010; Shima et al. 2020) synchronize spawning with the moon to increase fecundation, disperse offspring

\*Correspondence: Daniel Ottmann, National Institute of aquatic Resources, Technical University of Denmark (DTU-Aqua), Kemitorvet 202, 2800 Kongens Lyngby, Denmark. danot@aqua.dtu.dk

This is an open access article under the terms of the Creative Commons Attribution License, which permits use, distribution and reproduction in any medium, provided the original work is properly cited.

Additional Supporting Information may be found in the online version of this article.

**Author Contribution Statement:** D.O. and Ø.F. designed the research. P.R. provided research funding. D.O., Ø.F., and T.L. designed the mechanistic models. D.O., P.R., and D.A.-B. collected field samples. D.A-B. curated field data. D.O. analyzed the field data. D.O. wrote the paper and all other authors edited the text and provided insights and comments.

with tidal currents, or minimize encounters with nocturnal predators.

Previous studies (Hernández-León 2008; Shima et al. 2021, 2022) hypothesized that some fishes whose larvae remain near the sea surface day and night synchronize spawning with lunar cycles to minimize offspring encounters with diel vertical migrants such as mesopelagic fish predators (e.g., lanternfishes). Mesopelagic fishes are the most abundant vertebrates on the planet (Irigoien et al. 2014), they live in the open ocean, and many of them migrate up and down in the water column in synchrony with surface light intensities (Benoit-Bird et al. 2009; Bianchi and Mislan 2016). This vertical migration allows them to maintain a relatively stable ambient light environment (Langbehn et al. 2019). At dusk, when it becomes too dark for their own predators to spot them, they rise closer to surface waters to feed. At dawn, they migrate back to depth. However, during full moon, surface light intensities are around three orders of magnitude higher than during new moon (starlit) nights (Kaartvedt et al. 2019). Therefore, mesopelagic fish halt their upward migration at greater depth during these periods, as it is no longer safe for them to migrate to the surface (Benoit-Bird et al. 2009; Prihartato et al. 2016). Although Shima's hypothesis that some fishes synchronize spawning with lunar cycles to minimize offspring encounters with diel vertical predators is appealing, it lacks empirical support because previous studies (Shima et al. 2021, 2022) were performed on coral reef fishes, whose synchrony with the

<sup>&</sup>lt;sup>2</sup>Centro Oceanográfico de Balears (IEO, CSIC), Palma de Mallorca, Spain

<sup>&</sup>lt;sup>3</sup>Department of Biological Sciences, University of Bergen, Bergen, Norway

moon may be masked by other processes driven by coastal tides, settlement to reefs, and nocturnal reef predators (Johannes 1978).

Changes in mesozooplankton biomass following the moon cycle can also favor survival of larvae that match their critical feeding period with the moon period when mesozooplankton is most abundant. This can occur in systems where full moon illumination pushes the night vertical position of large zooplankton deeper, reducing top-down predation on the mesozooplankton that remain near the surface (Pinot and Jansá 2001; Hernández-León 2008).

Here, we evaluate if Atlantic bluefin tuna Thunnus thynnus in the Mediterranean Sea synchronizes spawning with the lunar stage to reduce predation by mesopelagic fish on their offspring. Atlantic bluefin tuna (hereafter ABFT) is a large pelagic fish that spawns in warm oligotrophic waters in both sides of the Atlantic Ocean, in the Gulf of Mexico, Slope Sea, and the Mediterranean Sea (Richardson et al. 2016; Muhling et al. 2017). The environment at the spawning grounds facilitate a rapid development of their offspring in a low-predator environment, at the cost of starvation risk due to low food availability and high metabolic demands (Fiksen and Reglero 2021; Ottmann et al. 2021b). Spawning in the western Mediterranean Sea usually starts at the beginning of June and lasts until mid-July (Alemany et al. 2010) ( $\sim 1.5$  lunar cycles). Adults spawn in open pelagic waters and eggs and larvae always remain within or above the thermocline (top  $\sim 25$  m). This makes ABFT a good model species to test if spawning around full moon reduces predation from mesopelagic fish, because ABFT is unaffected by other processes driven by the moon, such as coastal tides, settlement to a substrate, or reef predators. Furthermore, there is no evidence that near-surface zooplankton abundance varies with the moon cycle in this oligotrophic area, as zooplankton dynamics are likely more driven by bottom-up processes related to productivity (Fernández de Puelles et al. 2007, 2014). As in other systems elsewhere, the community of mesopelagic fish in the study area conducts diel vertical migrations (Olivar et al. 2012), and includes species whose vertical position in the water column respond to ambient light intensity (Langbehn et al. 2019).

We apply two sets of mechanistic models to quantify how moon phases affect fitness of ABFT early life stages via its effect on predation intensity from mesopelagic fish. First, we build on our recent models of larval ABFT fitness as a function of water temperature, food availability, and invertebrate predators (Fiksen and Reglero 2021; Ottmann et al. 2021b), and second, we use the local ambient light in combination with other behavioral models (Langbehn et al. 2019; Ljungström et al. 2021) to predict optimal migration and foraging of mesopelagic fish. This lets us predict the effect of mesopelagic fish preying on ABFT early life stages and predict optimal spawning time in terms of survival from birth to a given body size. We then combine these models to predict survival chances of tuna eggs spawned at different times of the moon

cycle, each experiencing different combinations of encounter rates and predator overlap as they hatch and grow larger. Finally, we compare predictions from the mechanistic model with long-term observations of tuna spawning to test if ABFT spawning intensity is affected by the lunar cycle. The combination of both (statistical and mechanistic) approaches allows us to suggest a causal nexus to statistical correlations observed between spawning activity and the moon cycle.

Natural mortality rates in early life stages of fish are highly variable and hard to measure. Thus, we do not expect to predict accurate values of survival (they may be wrong by several orders of magnitude). Instead, our goal is to evaluate how temporal cycles in larval fitness drive optimal spawning phenology of fishes. Therefore, even if the predicted change in larval fitness caused by mesopelagic fish is inaccurate, the direction and relative shift of the effect remains consistent.

#### Methods

## A mechanistic model of growth and survival of early life stages in ABFT

Temporal variation in the environment affects feeding and growth rates, as well as the predation risk of fish early life stages. This creates cycles in expected fitness of eggs and larvae born at different times, and thus optimal spawning phenology. We define larval fitness  $F_P$  (dimensionless) as the probability that an ABFT egg released at a given date and hour will hatch  $H_{\rm E}$ , grow, and survive during the time it takes to develop from an egg to a larva of 7.5 mm standard length (SL; Reglero et al. 2018; Fiksen and Reglero 2021). We model two sources of mortality from which we have empirical and experimental data—and find survival probabilities given densities of mesopelagic fish  $S_{P,M}$ , and seasonal invertebrate predators  $S_{P,I}$ . We include all other sources of size-dependent background mortality (as survival probability S<sub>P.B</sub>) using McGurk's (1986) empirical model for fish eggs and larvae, adapted by Fiksen and Reglero (2021) to ABFT early life stages in the Mediterranean Sea (see details in Supplementary Methods SM2):

$$F_{P} = H_{E} \cdot S_{P,I} \cdot S_{P,M} \cdot S_{P,B} \tag{1}$$

At a body length of 7.5 mm, ABFT larvae complete the notochordal flexion and become predominantly piscivorous (Blanco et al. 2018). In the mechanistic individual-based model (*see* details in Supplementary Methods SM1, SM2), we release an egg every hour of the year to calculate fitness at any potential spawning time as a direct function of the environmental conditions. Then, we identify the spawning time that maximizes fitness.

The environmental drivers include water temperature from historical records, number of daylight hours and light intensity from the sun and the moon obtained from the ESOP2 version of the Miami Isopycnic Coordinate Ocean Model (MICOM) and lunar irradiance estimates (Denton 1990;

Drange and Simonsen 1996), and ABFT prey (nauplii and Cladocera) and predator (mesopelagic fish and seasonal invertebrates) densities resolved to an hourly scale over the annual cycle (Fig. 1). All these variables are derived from empirical observations and are detailed in Supplementary Methods SM1. Light attenuation is calculated with local measurements of light in the water column. Cladocera densities are interpolated from monthly observations in a field station inshore of the spawning grounds (Fernández de Puelles et al. 2007; Atienza et al. 2016) and scaled for the depth distribution and reduced concentrations with distance offshore (Fiksen and Reglero 2021). Also, based on similar combinations of timeseries inshore and surveys in the spawning area the nauplii density is held constant through the season at 400 ind.  $m^{-3}$ , as a typical value. While we assume that the abundance of nauplii is not affected by moon cycles in our study area, other studies elsewhere have found that near-surface mesozooplankton abundance follows circalunar patterns (Hernández-León 2002). We therefore add a sensitivity analysis comparing larval fitness in conditions where nauplii abundance is constant vs. following circalunar fluctuations (see Supplementary Methods SM1).

Growth and development of eggs and larvae is modeled following Fiksen and Reglero (2021) and depends on water temperature and daily feeding activity (larval ABFT only feed during the day, as it is too dark at night for them to see (Hilder et al. 2017, 2019). Further details and equations can be found in Supplementary Methods SM2. We model ABFT feeding as a visual predator with a type II functional response using measured values of visual acuity (Hilder et al. 2019) and swimming speeds (Reglero et al. 2015). Total mortality of ABFT is the combined predation from invertebrates, mesopelagic fish, and all other sources. We model predation from seasonal invertebrates as represented by the jellyfish Pelagia noctiluca, which is considered the most important invertebrate predator of ABFT eggs and larvae in the study region and have seasonal changes in abundance (Gordoa et al. 2013; Ottmann et al. 2021b). We model them as passive predators with Holling type I functional response (see Ottmann et al. 2021b), using local abundances of P. noctiluca metaephyrae from surveys in the Balearic Seas (Supplementary Table S2) (Ottmann et al. 2021a) and their clearance rate obtained in laboratory experiments by Gordoa et al. (2013).

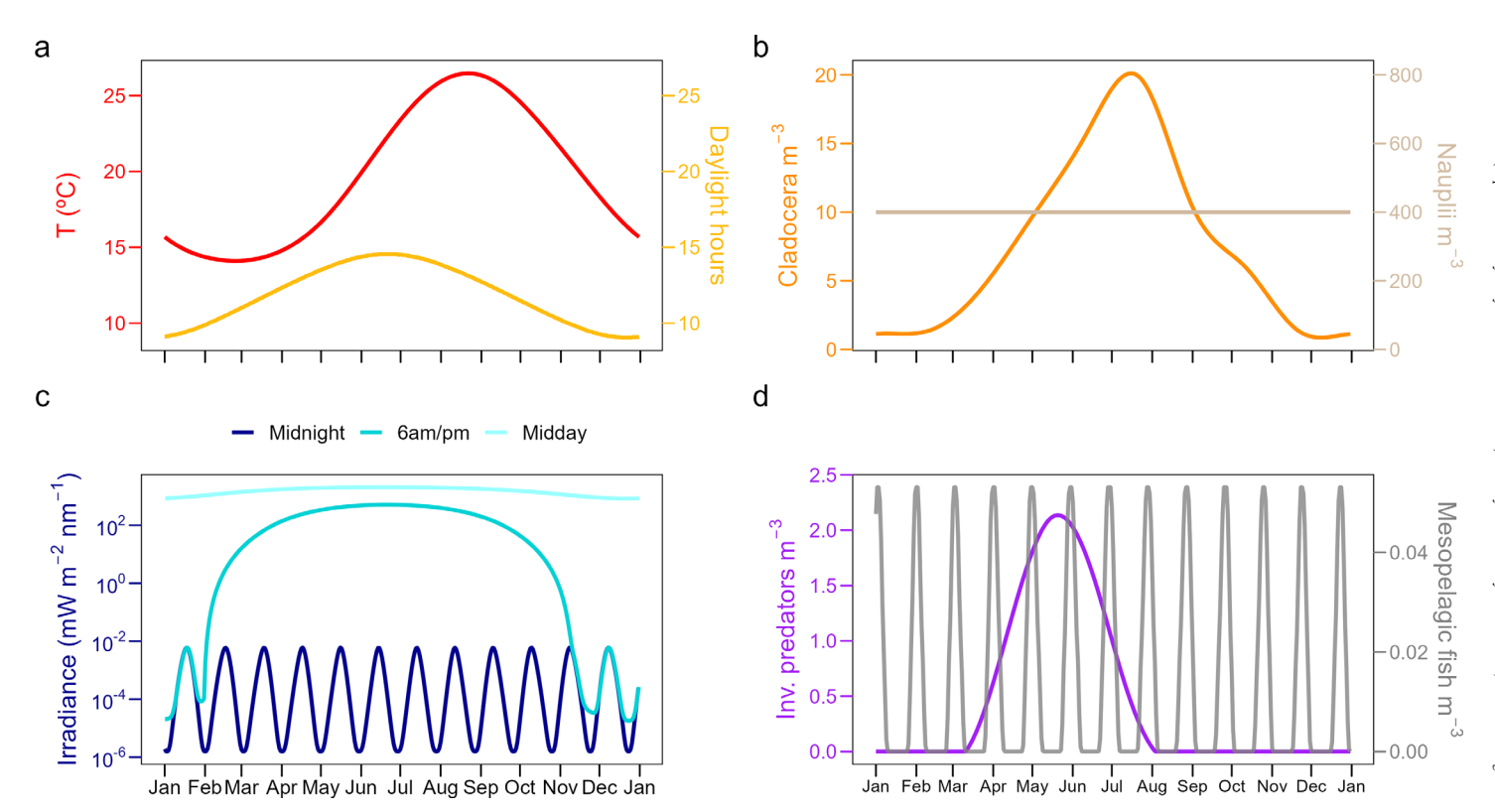


**Fig. 1.** Simulated environment over a 1-yr period (*see* "Methods" section) for offshore ABFT in the Balearic Islands spawning ground. (**a**) Sea-surface water temperature (°C), and number of daylight hours where the combined irradiance of the sun and the moon enable ABFT larvae to feed effectively (≥ 2.17 mW m<sup>-2</sup> nm<sup>-1</sup> at 486 nm); (**b**) ABFT prey density (individuals m<sup>-3</sup>); cladocerans and nauplii. Nauplii are held constant at 400 ind m<sup>-3</sup>; (**c**) Sea surface irradiance (mW m<sup>-2</sup> nm<sup>-1</sup>) at midday, midnight and 6 am/pm with clear sky. Lunar cycles, seen most strongly in the dark blue line, follow the 2022 calendar; (**d**) Density (individuals m<sup>-3</sup>) of ABFT invertebrate and mesopelagic fish predators. Nightly maxima of mesopelagic fish near the surface (where ABFT larvae are found) are inversely related to the moon phase.

Mesopelagic fish are modeled as Holling type II visual predators, and placed in their predicted light comfort zone (Langbehn et al. 2019) driven by the sun and lunar cycle. We parameterize the mesopelagic fish to resemble the myctophid Bentosema glaciale. While the response of other mesopelagic fish to ambient light is not as well characterized as for B. glaciale, previous studies show that vertical positioning in response to ambient light is widespread in scattering layers containing mesopelagic fishes (Bianchi and Mislan 2016; Aksnes et al. 2017; Kaartvedt et al. 2019) and that local species conduct diel vertical migration (Olivar et al. 2012). We use densities estimated in surveys for local mesopelagic fishes that include fish larvae in their diet. Olivar et al. (2012) estimated summer abundance of mesopelagic fishes in offshore (slope) areas around the Balearic Islands by towing a mesopelagic trawl at the deep scattering layer. Among the species that feed on fish early life stages (Bernal et al. 2015), Benthosema glaciale, Hygophum benoiti, Hygophum hygomii, Myctophum punctatum, Ceratoscopelus maderensis, Lampanictus crocodilus, Lobianchia dofleini, and Notoscopelus elegantus were the most abundant and had an estimated combined density of 0.0061 ind m<sup>-3</sup> in the near-surface scattering layer. However, we increase this value by one order of magnitude, because Kaartvedt et al. (2012) showed that mesopelagic trawls underestimate real abundances by about one order of magnitude.

Finally, we calculate the effect of other (less understood) sources of mortality including other predators and diseases using a statistical size-dependent mortality function (McGurk 1986) scaled to ABFT early life stages in the Mediterranean Sea (Fiksen and Reglero 2021).

### Analysis of field observations to find ABFT spawning time within the lunar cycle

We compare the model predictions with spawning intensity in the western Mediterranean Sea using ABFT larvae from 1928 ichthyoplankton samples collected from 2001 to 2020 and the respective environmental and lunar data. We applied a pre-developed larval index (Alvarez-Berastegui et al. 2020) that reflects the spawning activity derived from larval abundances in the spawning ground (see Supplementary Methods SM3 for further details). The larval index is, in essence, a bayesian hurdle-gamma generalized additive model (GAM) that evaluates standardized larval presence (hurdle part of the model) and abundance (positive part of the model) as a function of environmental conditions. Water temperature and salinity are key environmental variables for where and when ABFT spawn (Ingram et al. 2017). As explanatory variables, we use geographic position Lon\_lat, year as a factor Year, normalized hour of the day Hour\_norm, day of the year Day, temperature residuals of the mixed layer Temp\_res, salinity anomaly of the mixed layer S\_anom. We further include lunar phase at the time of spawning as an additional variable in the GAM to evaluate how moon phase affects spawning intensity.

$$Y_{L} = \beta_{0} + Year + s_{1}(Lon\_lat) + s_{2}(Hour\_norm) + s_{3}(Day) + s_{4}(Temp\_res) + s_{5}(S\_anom) + s_{6}(Moon\_phase) + \varepsilon$$
 (2)

Here,  $Y_L$  are captures per unit effort (standardized larvae  $m^{-2}$ ),  $\beta_0$  is the intercept,  $s_{1-6}$  are each for the smoothing parameters, and  $\varepsilon$  is the model error. The smoothing parameter of environmental variables are restricted to three knots to prevent overfitting the model. Temperature residuals are computed for each year from the linear temperature increase over the season, and salinity anomaly is standardized to the annual mean salinity (see Alvarez-Berastegui et al. 2020 for further details of the model). Lunar phase at the time of spawning is back-calculated from mean larval size (corrected as in Ottmann et al. 2022 for formalin shrinkage) applying temperature-dependent equations for egg and larval development rates (see Supplementary Methods SM3 for details and limitations of this approach). This enables us to identify the lunar phases when ABFT spawns most or least actively and compare it with the model predictions of larval fitness.

#### Results

## Predicted survival and optimal spawning times with moon phases and mesopelagic predators

Figure 2 shows the modeled chance that an egg survives from the time it is spawned until it hatches (egg survival; Fig. 2b) and then until it becomes a larva of 7.5 mm SL (larval fitness; Fig. 2c,d). The growth and development rates are functions of habitat conditions at the spawning ground. If there is no effect of mesopelagic fish predators (black line in Fig. 2c,d), the model predicts that, in an average year, an egg is viable between the beginning of June and the second week of July (Fig. 2c). The onset of the spawning window is triggered by a rise in water temperature, where 19°C is the minimum temperature for eggs to hatch (Reglero et al. 2018). As the season progresses, the water temperature keeps rising, accelerating egg hatching and larval growth rate. At the beginning, faster development increases larval fitness because it shortens the time they are exposed to predators and other sources of mortality. However, faster growth needs to be matched with sufficient energy supply. When the temperature rises above a certain threshold, larval metabolic demands exceed the energy supplied by available food and larvae starve (abrupt drop of fitness in Fig. 2c,d). As a result of this food-temperature tradeoff, larval fitness increases asymptotically across the spawning window until collapsing at the metabolic breakpoint around 04 July (Fig. 2c).

Model predictions show that predation by mesopelagic fishes can disrupt the pattern described above and reduce larval fitness by up to two orders of magnitude when spawning coincides with new moon and mesopelagic fish migrate closest to the surface (shown for 2 yr in Fig. 2c, blue and orange lines). Highest predation by mesopelagic fish occurs at nights around new moon, as illustrated by the drop in egg survival.

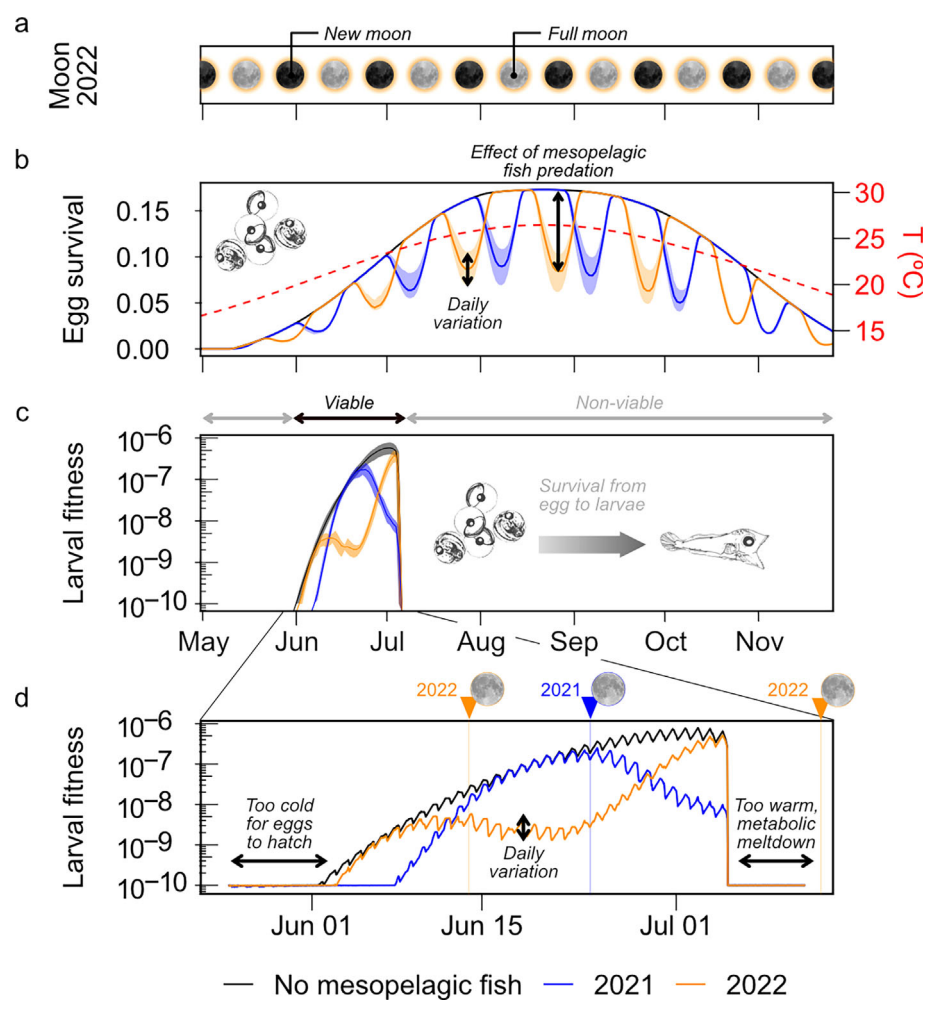


**Fig. 2.** Modeled larval fitness (survival from egg to metamorphosis at a larva of 7.5 mm SL) over time in relation to the moon phase. (a) Moon phases in 2022. Moon phases in 2021 (not shown) differed by 11 d. (b) Egg survival from spawning to the time of hatching; (c) larval fitness; (d) larval fitness zoomed in the window of viable spawning. Solid lines indicate daily (b, c) and hourly (d) values; shading in (b) and (c) indicate daily variation; black color shows the model output assuming there is no effect of mesopelagic fish predators; blue and orange colors show the model output with the lunar calendars of 2021 and 2022, respectively, with all other environmental variables kept the same; red, dashed line is water temperature (°C); vertical lines in (d) indicate full moon.

However, the cumulative effect of predation on eggs, yolk-sack, and pre-flexion larvae (Fig. 2c,d, blue and orange lines) show that eggs released within the week before new moon experience the greatest loss of fitness. Eggs released within the week before full moon, however, experience minimal loss of fitness. If moon phases shift across years and we assume all other environmental variables remain the same, the optimal spawning time varies from year to year because it fosters a different match with other variables like water temperature and food availability (Fig. 2c blue and orange lines).

Within each day, eggs spawned at different times of the day have different fitness depending on the combined effect of mesopelagic fish predation and the time of day for first feeding (Fig. 2d, small wiggles in the lines). Individuals hatched at the beginning of the night experience greater

cumulative predation by mesopelagic fish, reducing their fitness. Individuals that morph from yolk-sack to feeding larva in the morning have an entire day to feed and grow, increasing their fitness relative to individuals that morph later in the day or at night. Both these effects are modulated by temperature and food availability, as they determine how fast eggs and larvae develop. For instance, under the conditions simulated for 2022, the optimal spawning time is 04 July at 08:00 local time. However, if we increase nauplii density from 400 to 500 nauplii m<sup>-3</sup> and keep all other variables the same, optimal spawning is postponed to the 12 July at 01:00 local time (Supplementary Fig. S5c). This occurs because greater food abundance will enable larvae to grow faster under the higher temperatures later in the season before running into metabolic meltdown.

Model of optimal phenology in tuna

### Observed spawning times in relation to moon phases

The analysis of two decades of field data with the larval index (GAM model) reveals that ABFT spawn throughout the entire moon cycle, but they do so more actively during the bright phase, peaking about 3 d before full moon and dipping about 3 d before new moon (Fig. 3). The selected model includes moon phase as an important variable for spawning intensity (positive part of the model), but not for presence/absence of spawning activity (hurdle part of the model). As found previously (Alvarez-Berastegui et al. 2020), the model also identifies other important variables affecting spawning behavior. This includes water temperature, in both the positive and hurdle parts of the model, and day-of-year and salinity anomaly in the hurdle part of the model (Supplementary Figs. S10, S11).

### Discussion

Mesopelagic fish are the most numerous vertebrates on Earth, but their effect as predators of other fish eggs and larvae is poorly understood. Our results suggest that synchronizing spawning with the lunar cycle increases offspring fitness of a pelagic fish, the Atlantic bluefin tuna, due to decreased predation by mesopelagic fish on eggs and larvae. The mechanistic model predicts that mesopelagic fish predators can reduce

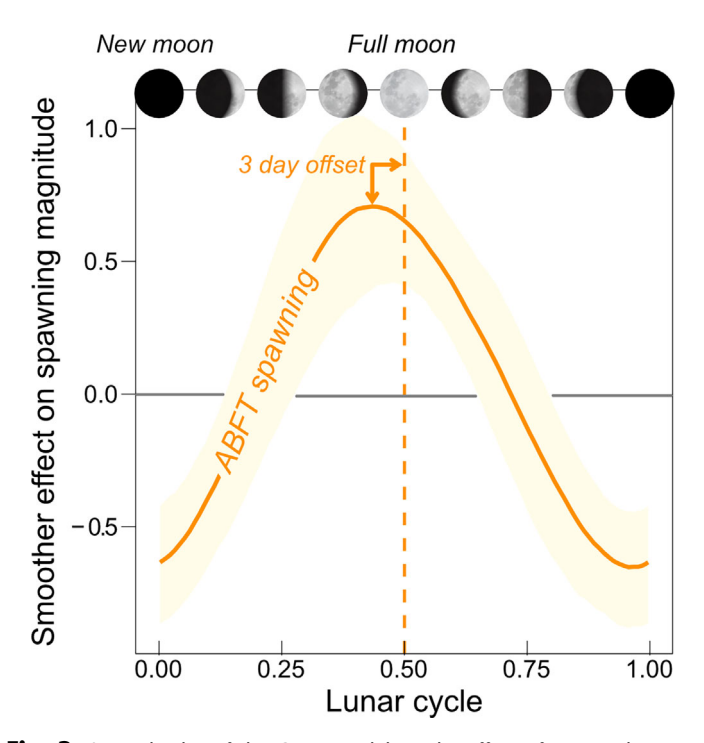


**Fig. 3.** Smooth plot of the GAM model on the effect of moon phase on ABFT spawning intensity, where 0 and 1 in the *x*-axis are new moon and 0.5 (dashed line) is full moon. Smoother values higher or lower than 0 (horizontal line) represent positive and negative effects of moon phase on spawning intensity. The shaded area is the standard error around the estimated smooth function.

larval fitness of ABFT by up to two orders of magnitude compared to a hypothetical scenario where mesopelagic fish were absent. However, it is the match between lunar phases with favorable conditions for growth and development that ultimately determines the optimal time for spawning within the viable window. Such match/mismatch conditions vary across years because the moon phase shifts by almost 11 d forwards from year to year, while the environment during the spawning window is more consistent from year to year (Fig. 2c). We have contrasted our mechanistic model with a long-term observational dataset that accommodates spatiotemporal variability of the habitat and multiple lunar calendars. Compared to other studies (Gordoa and Carreras 2014: Shimose et al. 2018), such long-term dataset strengthens the robustness of our statistical analysis. Results of this statistical analysis show that spawning intensity match the optimal spawning time predicted by the mechanistic model, lending support to the hypothesis that predation by mesopelagic fish is a driver of lunar synchrony in fish spawning.

The mechanistic model predicts that the best and worst times for spawning are within the week before full moon or new moon, respectively. This timing occurs because eggs released within the week before full moon and new moon will accumulate less and more time of exposure to mesopelagic fish predation, respectively, before being able to evade them. Among years with different lunar calendar, the exact day of optimal spawning before full moon depends on the match/ mismatch of the optimal lunar phase with the other variables that we assume follow the same seasonal pattern between years (water temperature, hours of daylight, food availability and abundance of invertebrate predators). The data analysis supports the model predictions by showing a clear cyclic pattern of spawning synchronized with the lunar cycle, where spawning intensity peaks 3 d before full moon, and lowest 3 d before new moon. These results are in line with previous observations of egg production in captured individuals (Gordoa and Carreras 2014) and match our model predictions.

Synchronized spawning activity with lunar cycles can be explained by natural selection. Eggs released at times that reduce predation by mesopelagic fish have a greater chance to survive and carry genetic information to future generations, propelling synchronous spawning with the moon to increase larval fitness. Because mesopelagic fish are abundant and ubiquitous in most pelagic systems (Irigoien et al. 2014; Proud et al. 2017), the patterns observed here should in theory be a widespread adaptation among fishes with pelagic eggs elsewhere, including top predator fishes. This mechanism can be further reinforced if fish eggs and larvae are preyed on by other diel vertical migrants whose migratory behavior is affected by lunar cycles (Pinot and Jansá 2001; Last et al. 2016). However, fishes can synchronize spawning with the moon for several reasons (Hernández-León 2008; Shima et al. 2021). For reef fishes, spawning synchrony with the moon has been proposed in relation to other lunar-related

processes, such as tides or encounters with visual predators at the time of settling to reefs (Demartini 1981; Sponaugle and Cowen 1996; Rankin and Sponaugle 2014). These other processes can potentially outweigh the effect of vertically migrant predators on larval fitness, and spawning synchrony may differ from that predicted by our model (Claydon et al. 2014). Circalunar fluctuations on the abundance of food availability can have a similar effect on larval fitness as mesopelagic fish predators, where offspring released the week before full moon experience optimal fitness, while offspring released the 2 weeks after full moon experience the greatest loss of fitness (Supplementary Fig. S6). In systems where mesozooplankton abundance follows circalunar fluctuations, the converge of both these processes can foster a stronger synchrony of fish spawning towards the days before full moon (Hernández-León 2002, 2008).

Pelagic fishes may synchronize spawning with the moon to reduce predation from mesopelagic fish and other diel vertical migrants. However, the few studies that have investigated synchronic spawning patterns of pelagic fish with moon phases would often require longer datasets or stronger statistics to obtain conclusive results (Farris 1963; Gordoa Carreras 2014; Shimose et al. 2018; Tanaka et al. 2020). Daily measurements of spawning over 2 yr showed that yellowfin tuna Thunnus albacares spawns most intensively the week before full moon (Margulies et al. 2007), as predicted also in our model. Post et al. (1997) found that sailfish larvae Istiophorus platypterus were less abundant in the first quarter moon, suggesting less spawning activity around new moon. However, Schlenker et al. (2021) concluded that mahi-mahi Coryphaena hyppurus spawned more actively around new moon. Regarding nearshore pelagic fishes (less exposed to mesopelagic predators than open ocean fishes). Spanish mackerel Scomberomorus maculatus spawns more actively around full moon (Tobin et al. 2014) and jack mackerel Trachurus declivis spawns more actively around full and new moon (Jordan 1994). Several reasons may explain why other pelagic species do not necessarily synchronize spawning with lunar phases as described in this study: different vertical position of eggs and larvae where they are exposed to mesopelagic fish throughout all the moon cycle, presence of other predators with smaller diel vertical migrations that permanently overlap with the fish early lie stages, more turbid water that alter the vertical preference of mesopelagic fishes, greater cloud coverage in spawning grounds elsewhere that increase stochasticity of night time illumination, courtship behavior synchronized with other environmental conditions that override lunar synchrony of spawning, and so on. Further long-term field studies are needed to identify predominant patterns of lunar spawning synchrony of pelagic species.

Contrary to the cases mentioned above, eels *Anguilla* spp. spawn during new moon and at depths that range 150–200 m (Tsukamoto et al. 2011; Ayala and Munk 2018). The reason for this remains unknown, but we suggest an analogous

hypothesis to our findings with ABFT. In nights around new moon, mesopelagic fish migrate from depth to surface waters, limiting predation to short periods of time in dusk and dawn, when mesopelagic fish pass through the depth where eel early life stages are. However, moon light around full moon pushes mesopelagic fish down to depths where they overlap with eel early life stages throughout the night. By spawning around new moon and at depths deeper than 150 m (Tsukamoto et al. 2011; Ayala and Munk 2018), eel can reduce spatial and temporal overlap of its eggs with mesopelagic fish and increase its fitness.

Adding cloud coverage as a variable in our statistical analyses could have improved its accuracy. However, clouds only cover > 50% of the sky for 11%-18% of the time during the spawning season of ABFT (Gelaro et al. 2017). Thus, we believe cloud coverage would not have altered the main finding of this study. The statistical model has produced a clear circalunar pattern of spawning activity indicating that the sample size (1928 sampling stations across 17 spawning seasons) was powerful enough to reveal a significant pattern despite using averaged estimates of larval age (see Methods). Similarly, the mechanistic model does not consider interannual or spatial variation of the environment. Instead, it represents the expected average fitness of tuna under a particular lunar calendar. Thus, using such large database accommodates the habitat variation of the spawning ground and enables to predict the average spawning activity in relation to the moon phase. Finally, a finer taxonomical resolution of mesopelagic fish diets and vertical response to light intensity would improve accuracy of our predictions and help identify major players among ABFT predators.

We have identified a mechanism whereby predation from mesopelagic fish may drive natural selection on other pelagic fishes towards synchronizing spawning with bright moon nights to reduce encounters of eggs and larvae with mesopelagic fish predators. This finding unveils a largely ignored matter, namely, the effect that the most abundant fish group on earth has on phenological adaptations of other fishes. Given the widespread abundance of mesopelagic fish in the global oceans, future studies on spawning phenology and larval ecology should consider mesopelagic fish as potentially important predators.

### Data availability statement

The data and R code supporting the results are archived in GitHub: <a href="https://github.com/dottmann/moon\_light">https://github.com/dottmann/moon\_light</a> and will be stored in Zenodo upon acceptance.

### References

Aksnes, D. L., A. Røstad, S. Kaartvedt, U. Martinez, C. M. Duarte, and X. Irigoien. 2017. Light penetration structures the deep acoustic scattering layers in the global ocean. Sci. Adv. **3**: e1602468. doi:10.1126/sciadv.1602468

- Alemany, F., and others. 2010. Characterization of the spawning habitat of Atlantic bluefin tuna and related species in the Balearic Sea (western Mediterranean). Prog. Ocean. **86**: 21–38. doi:10.1016/j.pocean.2010.04.014
- Alvarez-Berastegui, D., M. P. Tugores, D. Ottmann, M. Martín-Quetglas, and P. Reglero. 2020. Bluefin tuna larval indices in the western Mediterranean, ecological and analytical sources of uncertainity. Collect. Vol. Sci. Pap. ICCAT **77**: 289–311.
- Atienza, D., A. Sabatés, S. Isari, E. Saiz, and A. Calbet. 2016. Environmental boundaries of marine cladoceran distributions in the NW Mediterranean: Implications for their expansion under global warming. J. Mar. Syst. **164**: 30–41. doi:10.1016/j.jmarsys.2016.08.003
- Ayala, D. J., and P. Munk. 2018. Growth rate variability of larval European eels (*Anguilla Anguilla*) across the extensive eel spawning area in the southern Sargasso Sea. Fish. Oceanogr. **27**: 525–535. doi:10.1111/fog.12273
- Benoit-Bird, K. J., W. W. L. Au, and D. W. Wisdoma. 2009. Nocturnal light and lunar cycle effects on diel migration of micronekton. Limnol. Oceanogr. **54**: 1789–1800. doi:10. 4319/lo.2009.54.5.1789
- Bernal, A., M. P. Olivar, F. Maynou, and M. L. Fernández de Puelles. 2015. Diet and feeding strategies of mesopelagic fishes in the western Mediterranean. Prog. Oceanogr. **135**: 1–17. doi:10.1016/j.pocean.2015.03.005
- Bianchi, D., and K. A. S. Mislan. 2016. Global patterns of diel vertical migration times and velocities from acoustic data: Global patterns of diel vertical migration. Limnol. Oceanogr. **61**: 353–364. doi:10.1002/lno.10219
- Blanco, E., P. Reglero, A. Ortega, F. de la Gándara, and A. Folkvord. 2018. Size-selective mortality of laboratory-reared Atlantic bluefin tuna larvae: Evidence from microstructure analysis of otoliths during the piscivorous phase. J. Exp. Mar. Biol. Ecol. **509**: 36–43. doi:10.1016/j.jembe.2018.08.009
- Claydon, J. A. B., M. I. McCormick, and G. P. Jones. 2014. Multispecies spawning sites for fishes on a low-latitude coral reef: Spatial and temporal patterns: Reef fish spawning sites. J. Fish Biol. **84**: 1136–1163. doi:10.1111/jfb.12355
- Demartini, E. E. 1981. Ovarian cycling frequency and batch fecundity in the queenfish, *Seriphus politus*: Attributes representative of serial spawning fishes. Fish. Bull. **79**: 547–560.
- Denton, E. 1990. Light and vision at depths greater than 200 metres, p. 127–248. *In* Light and live in the sea. Cambridge Univ. Press.
- Drange, H., and K. Simonsen. 1996. Formulation of air–sea fluxes in the ESOP2 version of MICOM. Nansen Environmental and Remote Sensing Center.
- Farris, D. A. 1963. Reproductive periodicity in the sardine (*Sardinops caerulea*) and the jack mackerel (*Trachurus symmetricus*) on the Pacific coast of North America. Copeia **1963**: 182. doi:10.2307/1441307
- Fernández de Puelles, M. L., F. Alemany, and J. Jansá. 2007. Zooplankton time-series in the Balearic Sea (Western

- Mediterranean): Variability during the decade 1994–2003. Prog. Oceanogr. **74**: 329–354. doi:10.1016/j.pocean.2007.04.009
- Fernández de Puelles, M. L., V. Macias, L. Vicente, and J. C. Molinero. 2014. Seasonal spatial pattern and community structure of zooplankton in waters off the Baleares archipelago (Central Western Mediterranean). J. Mar. Syst. **138**: 82–94. doi:10.1016/j.jmarsys.2014.01.001
- Fiksen, Ø., and P. Reglero. 2021. Atlantic bluefin tuna spawn early to avoid metabolic meltdown in larvae. Ecology **103**: 1–8. doi:10.1002/ecy.3568
- Fryer, G. 1986. Ecology: Lunar cycles in lake plankton. Nature **322**: 306. doi:10.1038/322306a0
- Gelaro, R., and others. 2017. The modern-era retrospective analysis for research and applications, version 2 (MERRA-2). J. Climate **30**: 5419–5454. doi:10.1175/JCLI-D-16-0758.1
- Gordoa, A., J. L. Acuña, R. Farrés, and K. Bacher. 2013. Burst feeding of *Pelagia noctiluca* ephyrae on Atlantic bluefin tuna (*Thunnus thynnus*) eggs. PloS One **8**: e74721. doi:10.1371/journal.pone.0074721
- Gordoa, A., and G. Carreras. 2014. Determination of temporal spawning patterns and hatching time in response to temperature of Atlantic bluefin tuna (*Thunnus thynnus*) in the Western Mediterranean. PLoS One **9**: e90691. doi:10.1371/journal.pone.0090691
- Hernández-León, S. 2002. Lunar cycle of zooplankton biomass in subtropical waters: Biogeochemical implications. J. Plankton Res. **24**: 935–939. doi:10.1093/plankt/24.9.935
- Hernández-León, S. 2008. Natural variability of fisheries and lunar illumination: A hypothesis. Fish Fish. **9**: 138–154. doi:10.1111/j.1467-2979.2008.00272.x
- Hilder, P. E., J. M. Cobcroft, and S. C. Battaglene. 2017. Factors affecting the feeding response of larval southern bluefin tuna, *Thunnus maccoyii* (Castelnau, 1872). Aquacult. Res. **48**: 2752–2766. doi:10.1111/are.13108
- Hilder, P. E., S. C. Battaglene, N. S. Hart, S. P. Collin, and J. M. Cobcroft. 2019. Retinal adaptations of southern bluefin tuna larvae: Implications for culture. Aquaculture **507**: 222–232. doi:10.1016/j.aquaculture.2019.04.024
- Ingram, G. W., D. Alvarez-Berastegui, P. Reglero, R. Balbín, A. García, and F. Alemany. 2017. Incorporation of habitat information in the development of indices of larval bluefin tuna (*Thunnus thynnus*) in the western Mediterranean Sea (2001–2005 and 2012–2013). Deep-Sea Res. II Top. Stud. Oceanogr. **140**: 203–211. doi:10.1016/j.dsr2.2017.03.012
- Irigoien, X., and others. 2014. Large mesopelagic fishes biomass and trophic efficiency in the open ocean. Nat. Commun. **5**: 3271. doi:10.1038/ncomms4271
- Jetz, W., J. Steffen, and K. E. Linsenmair. 2003. Effects of light and prey availability on nocturnal, lunar and seasonal activity of tropical nightjars. Oikos **103**: 627–639. doi:10. 1034/j.1600-0706.2003.12856.x
- Johannes, R. E. 1978. Reproductive strategies of coastal marine fishes in the tropics. Environ. Biol. Fishes **3**: 65–84. doi:10. 1007/BF00006309

- Jordan, A. 1994. Age, growth and back-calculated birthdate distributions of larval jack mackerel, *Trachurus declivis* (Pisces: Carangidae), from eastern Tasmanian coastal waters. Mar. Freshw. Res. **45**: 19. doi:10.1071/MF9940019
- Kaartvedt, S., A. Staby, and D. Aksnes. 2012. Efficient trawl avoidance by mesopelagic fishes causes large underestimation of their biomass. Mar. Ecol. Prog. Ser. **456**: 1–6. doi:10. 3354/meps09785
- Kaartvedt, S., T. J. Langbehn, and D. L. Aksnes. 2019. Enlightening the ocean's twilight zone. ICES J. Mar. Sci. **76**: 803–812. doi:10.1093/icesjms/fsz010
- Kronfeld-Schor, N., D. Dominoni, H. de la Iglesia, O. Levy,
  E. D. Herzog, T. Dayan, and C. Helfrich-Forster. 2013.
  Chronobiology by moonlight. Proc. R. Soc. B 280: 20123088. doi:10.1098/rspb.2012.3088
- Langbehn, T., D. Aksnes, S. Kaartvedt, Ø. Fiksen, and C. Jørgensen. 2019. Light comfort zone in a mesopelagic fish emerges from adaptive behaviour along a latitudinal gradient. Mar. Ecol. Prog. Ser. 623: 161–174. doi:10.3354/meps13024
- Last, K. S., L. Hobbs, J. Berge, A. S. Brierley, and F. Cottier. 2016. Moonlight drives ocean-scale mass vertical migration of zooplankton during the Arctic winter. Curr. Biol. **26**: 244–251. doi:10.1016/j.cub.2015.11.038
- Ljungström, G., T. J. Langbehn, and C. Jørgensen. 2021. Light and energetics at seasonal extremes limit poleward range shifts. Nat. Clim. Chang. **11**: 530–536. doi:10.1038/s41558-021-01045-2
- Margulies, D., J. Suter, S. Hunt, R. Olson, V. Scholey, J. Wexler, and A. Nakazawa. 2007. Spawning and early development of captive yellowfin tuna (*Thunnus albacares*). Fish. Bull. **105**: 249–265.
- McGurk, M. D. 1986. Natural mortality of marine pelagic fish eggs and larvae: Role of spatial patchiness. Mar. Ecol. Prog. Ser. **34**: 227–242. doi:10.3354/meps034227
- Mougeot, F., and V. Bretagnolle. 2000. Predation risk and moonlight avoidance in nocturnal seabirds. J. Avian Biol. **31**: 376–386. doi:10.1034/j.1600-048X.2000.310314.x
- Muhling, B. A., and others. 2017. Reproduction and larval biology in tunas, and the importance of restricted area spawning grounds. Rev. Fish. Biol. Fish. **27**: 697–732. doi: 10.1007/s11160-017-9471-4
- Neely, K. L., and C. B. Butler. 2020. Seasonal, lunar, and diel patterns in spawning by the giant barrel sponge, *Xestospongia muta*. Coral Reefs **39**: 1511–1515. doi:10.1007/s00338-020-02009-2
- Olivar, M. P., A. Bernal, B. Molí, M. Peña, R. Balbín, A. Castellón, J. Miquel, and E. Massutí. 2012. Vertical distribution, diversity and assemblages of mesopelagic fishes in the western Mediterranean. Deep Sea Res. I Oceanogr. Res. Pap. **62**: 53–69. doi:10.1016/j.dsr.2011.12.014
- Ottmann, D., D. Álvarez-Berastegui, L. Prieto, R. Balbín, F. Alemany, Ø. Fiksen, A. Gordoa, and P. Reglero. 2021a. Abundance of *Pelagia noctiluca* early life stages in the

- western Mediterranean Sea scales with surface chlorophyll. Mar. Ecol. Prog. Ser. **658**: 75–88. doi:10.3354/meps13423
- Ottmann, D., Ø. Fiksen, M. Martín, F. Alemany, and L. Prieto. 2021*b*. Spawning site distribution of a bluefin tuna reduces jellyfish predation on early life stages. Limnol. Oceanogr. **66**: 3669–3681. doi:10.1002/lno.11908
- Ottmann, D., P. Reglero, F. Alemany, D. Alvarez-Berastegui, M. Martín, and Ø. Fiksen. 2022. Small fish eat smaller fish: A model of interaction strength in early life stages of two tuna species. Limnol. Oceanogr. **7**: 227–234. doi:10.1002/lol2.10241
- Palmer, M. S., J. Fieberg, A. Swanson, M. Kosmala, and C. Packer. 2017. A "dynamic" landscape of fear: Prey responses to spatiotemporal variations in predation risk across the lunar cycle. Ecol. Lett. 20: 1364–1373. doi:10.1111/ele. 12832
- Pinot, J. M., and J. Jansá. 2001. Time variability of acoustic backscatter from zooplankton in the Ibiza Channel (western Mediterranean). Deep Sea Res. I Oceanogr. Res. Pap. **48**: 1651–1670. doi:10.1016/S0967-0637(00)00095-9
- Post, J. T., J. E. Serafy, T. R. Capo, and D. P. de Sylva. 1997. Field and laboratory observations on larval Atlantic sailfish (*Istiophorus platypterus*) and swordfish (*Xiphias gladius*). Bull. Mar. Sci. **60**: 1026–1034.
- Prihartato, P., X. Irigoien, M. Genton, and S. Kaartvedt. 2016. Global effects of moon phase on nocturnal acoustic scattering layers. Mar. Ecol. Prog. Ser. **544**: 65–75. doi:10.3354/meps11612
- Proud, R., M. J. Cox, and A. S. Brierley. 2017. Biogeography of the global ocean's mesopelagic zone. Curr. Biol. **27**: 113–119. doi:10.1016/j.cub.2016.11.003
- Prugh, L. R., and C. D. Golden. 2014. Does moonlight increase predation risk? Meta-analysis reveals divergent responses of nocturnal mammals to lunar cycles. J. Anim. Ecol. **83**: 504–514. doi:10.1111/1365-2656.12148
- Rankin, T. L., and S. Sponaugle. 2014. Characteristics of settling coral reef fish are related to recruitment timing and success. PLoS One **9**: e108871. doi:10.1371/journal.pone. 0108871
- Reglero, P., N. Zaragoza, E. Blanco, F. de la Gandara, A. P. Torres, and A. Ortega. 2015. Routine swimming speed of bluefin tuna larvae measured in the laboratory. Proceedings of the 39th Annual Larval Fish Conference, Vienna, 12–17 July 2015.
- Reglero, P., and others. 2018. Atlantic bluefin tuna spawn at suboptimal temperatures for their offspring. Proc. R. Soc. B Biol. Sci. **285**: 20171405. doi:10.1098/rspb.2017.1405
- Richardson, D. E., and others. 2016. Discovery of a spawning ground reveals diverse migration strategies in Atlantic blue-fin tuna (*Thunnus thynnus*). Proc. Natl. Acad. Sci. USA **113**: 3299–3304. doi:10.1073/pnas.1525636113
- Richmond, R., and C. Hunter. 1990. Reproduction and recruitment of corals: Comparisons among the Caribbean, the

Model of optimal phenology in tuna

- Tropical Pacific, and the Red Sea. Mar. Ecol. Prog. Ser. **60**: 185–203. doi:10.3354/meps060185
- Schlenker, L. S., and others. 2021. Remote predictions of mahi-mahi (*Coryphaena hippurus*) spawning in the open ocean using summarized accelerometry data. Front. Mar. Sci. 8: 626082. doi:10.3389/fmars.2021.626082
- Shima, J. S., C. W. Osenberg, S. H. Alonzo, E. G. Noonburg, P. Mitterwallner, and S. E. Swearer. 2020. Reproductive phenology across the lunar cycle: Parental decisions, offspring responses, and consequences for reef fish. Ecology **101**: e03086. doi:10.1002/ecy.3086
- Shima, J. S., C. W. Osenberg, E. G. Noonburg, S. H. Alonzo, and S. E. Swearer. 2021. Lunar rhythms in growth of larval fish. Proc. R. Soc. B Biol. Sci. **288**: 20202609. doi:10.1098/rspb.2020.2609
- Shima, J. S., C. W. Osenberg, S. H. Alonzo, E. G. Noonburg, and S. E. Swearer. 2022. How moonlight shapes environments, life histories, and ecological interactions on coral reefs. Emerg. Topic. Life Sci. **6**: 45–56. doi:10.1042/ETLS20210237
- Shimose, T., Y. Aonuma, T. Tanabe, N. Suzuki, and M. Kanaiwa. 2018. Solar and lunar influences on the spawning activity of Pacific bluefin tuna (*Thunnus orientalis*) in the south-western North Pacific spawning ground. Fish. Oceanogr. 27: 76–84. doi:10.1111/fog.12235
- Sponaugle, S., and R. Cowen. 1996. Nearshore patterns of coral reef fish larval supply to Barbados, West Indies. Mar. Ecol. Prog. Ser. **133**: 13–28. doi:10.3354/meps133013
- Takemura, A., M. S. Rahman, and Y. J. Park. 2010. External and internal controls of lunar-related reproductive rhythms in fishes. J. Fish Biol. **76**: 7–26. doi:10.1111/j.1095-8649. 2009.02481.x
- Tanaka, H., T. Kodama, N. Suzuki, Y. Mochizuki, H. Ashida, T. Sato, H. Takeshima, and K. Nohara. 2020. The distribution and early growth of juvenile Pacific bluefin tuna Thunnus orientalis around Sado Island in the eastern Sea of Japan. Fish Sci. **86**: 1019–1028. doi:10.1007/s12562-020-01470-w

- Tobin, A., M. Heupel, C. Simpfendorfer, J. Pandolfi, R. Thurstan, and S. Buckley. 2014. Utilising innovative technology to better understand Spanish mackerel spawning aggregations and the protection offered by marine protected areas. Spanish mackerel spawning aggregations and marine protected areas FRDC Project No 2010/007. FRDC Project No 2010/007. Centre for Sustainable Tropical Fisheries and Aquaculture, James Cook Univ.
- Tsukamoto, K., and others. 2011. Oceanic spawning ecology of freshwater eels in the western North Pacific. Nat. Commun. 2: 179. doi:10.1038/ncomms1174
- Žuljević, A., M. Despalatović, I. Cvitković, B. Morton, and B. Antolić. 2018. Mass spawning by the date mussel *Lithophaga lithophaga*. Sci. Rep. **8**: 10781. doi:10.1038/s41598-018-28826-8

### Acknowledgments

This work received funds from the European Union's Horizon 2020 research and innovation program under grant agreements No 773713 (PANDORA) and the the project Baleatun (grant agreement PDR2020/78) founded by the Balearic Government (Direcció General de Política Universitària i Recerca i de l'Impost del Turisme Sostenible). It was also supported by the Spanish Institute of Oceanography (EU Data Collection Regulation, Survey TUNIBAL) and its joined research initiative with the Balearic Islands Coastal Observing and Forecasting System (SOCIB) (BLUEFIN). D.O. was supported by the Independent Research Fund Denmark and by the FPI Fellowship from Vicepresidència i Conselleria d'Innovació, Recerca i Turisme of the regional Government of the Balearic Islands co-financed by the 2014–2020 European Social Fund program. T.J.L. received funding from the Research Council of Norway, project 294819.

### **Conflict of Interests**

None declared.

Submitted 19 August 2023 Revised 29 September 2023 Accepted 02 October 2023

Associate editor: Kelly J. Benoit-Bird